PostCam: Camera-Controllable Novel-View Video Generation with Query-Shared Cross-Attention

Yipeng Chen^{1*}, Zhichao Ye^{2*}, Zhenzhou Fang ¹, Xinyu Chen¹, Xiaoyu Zhang², Jialing Liu², Nan Wang², Haomin Liu^{2†}, Guofeng Zhang^{1†}

¹State Key Lab of CAD&CG, Zhejiang University ²Shanghai InSpatio Intelligent Technology Co., Ltd. *Equal Contribution, [†]Corresponding Authors

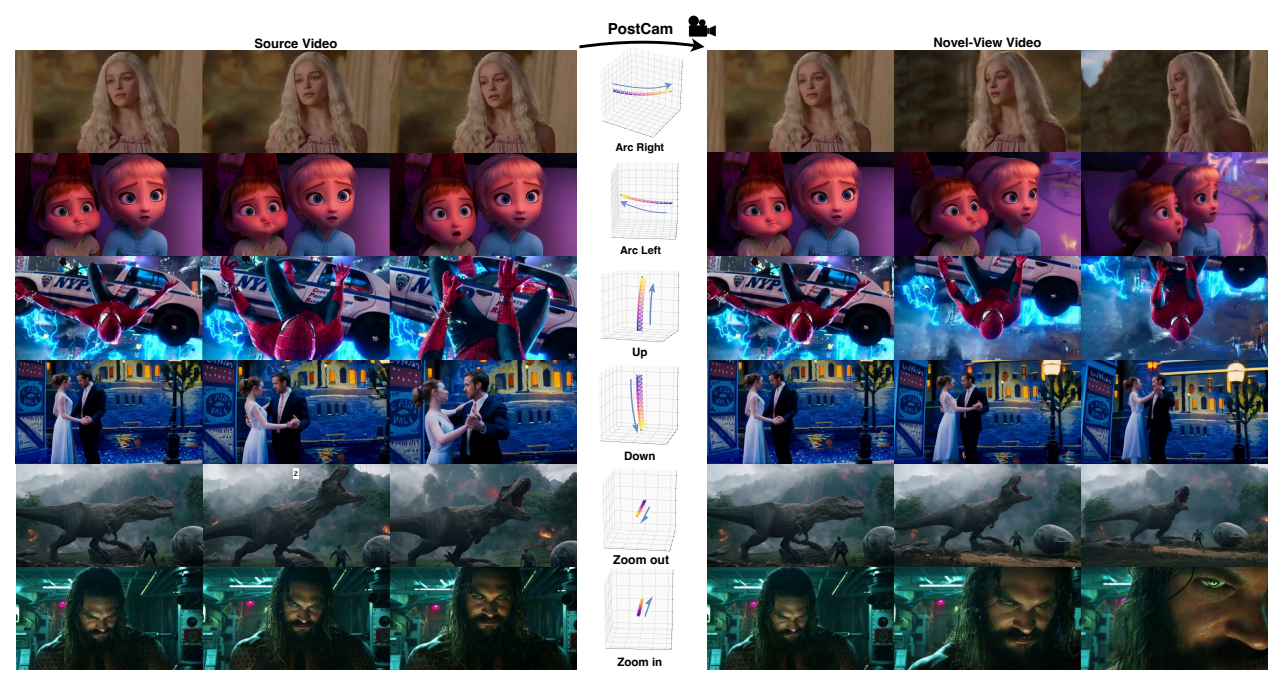


Figure 1. Given a source video (left) and a target camera trajectory (middle), PostCam generates high-quality novel-view videos (right), enabling post-capture editing of camera motion in dynamic scenes. Despite using a lightweight backbone with only 1.3B-parameters, PostCam achieves precise trajectory control and high-fidelity novel-view synthesis across a wide range of video styles and motion patterns.

Abstract

We propose PostCam, a framework for novel-view video generation that enables post-capture editing of camera trajectories in dynamic scenes. We find that existing video recapture methods suffer from suboptimal camera motion injection strategies—such suboptimal designs not only limit camera control precision but also result in generated videos that hardly to preserve fine visual details from the source video. To achieve more accurate and flexible motion manipulation, PostCam introduces a query-shared cross-attention module. It integrates two distinct forms of control signals:

the 6-DoF camera poses and the 2D rendered video frames. By fusing them into a unified representation within a shared feature space, our model can extract underlying motion cues, which enhances both control precision and generation quality. Furthermore, we adopt a two-stage training strategy: the model first learns coarse camera control from pose inputs, and then incorporates visual information to refine motion accuracy and enhance visual fidelity. Experiments on both real-world and synthetic datasets demonstrate that PostCam outperforms state-of-the-art methods by over 20% in camera control precision and view consistency, while achieving the highest video generation quality. Our project webpage is publicly available at: this https URL.



Figure 2. Comparison with State-of-the-Art Methods in Real Dynamic Scenes. We compare the last-frame results of state-of-the-art (SOTA) methods and our approach, with the last frame of the source video shown in the first column for reference. Across all examples, our method consistently preserves fine details (e.g., faces, hands), while SOTA methods often suffer from blurring, distortion, and identity drift. Moreover, our approach remains robust even in challenging cases where SOTA methods fail completely (rows 4–5), producing high-quality and temporally coherent results. For more comparisons, please refer to our supplementary videos.

1. Introduction

Recent years have witnessed remarkable progress in videogeneration models [6, 27, 32, 38, 44], with substantial improvements in both the fidelity and diversity of the generated results. Consequently, an increasing body of research has focused on controllable video generation, which seeks fine-grained control over video properties to accommodate the demands of diverse application scenarios. Among all video properties, camera motion is one of the most fundamental that alone charts the viewpoint trajectory through which we explore the virtual world generated by models. The film industry has long explored the camera language, a craft that shapes narrative focus and emotional rhythm while serving as a cornerstone of traditional production. However, most of camera motion effects rely on expensive hardware and specialized expertise, making them inaccessible to the majority of amateur creators. This work aims at camera-controllable novel-view video generation—given a reference video and an arbitrary camera trajectory, this task produces a spatiotemporally consistent video that enables post-capture editing of camera-motion. This task is a highly challenging scenario in controllable video generation, demanding temporal synchronization, spatial consistency, and reasonable inpainting of unobserved regions.

Although camera-controllable image-to-video (I2V)

generation has been extensively studied, research on camera-controllable video-to-video (V2V) generation remains largely underexplored. A representative method, Re-CameraMaster, encodes the camera trajectory into a camera embedding and directly injects it into the denoising tokens to achieve camera motion control. This approach, however, has limited generalization, often resulting in blurriness, identity drift, or even complete failure. In contrast, TrajectoryCrafter [24] adopts a rendering-based strategy: it first lifts the source video into a 3D point cloud via monocular depth estimation, then renders the video according to the target camera pose to provide stronger visual information. Its performance is highly sensitive to depth estimation accuracy—any estimation errors can cause artifacts or texture drifting, ultimately degrading the overall video quality. Additionally, some image-to-video works, such as MVGen-Master [7] and Uni3C [8], explore simple modality fusion schemes. They typically combine Plücker coordinates (derived from camera poses) with rendered videos via additive and channel concatenation in the latent space. Nevertheless, we find that these fusion strategies remain suboptimal, making it difficult to preserve fine-grained details from the reference video in the generated results.

We introduce PostCam, a camera-controllable novelview video generation framework that enables post-capture editing of camera motion along arbitrary user-defined tra-Its key innovation is a query-shared crossattention module, which integrates two conditional modalities, 6-DoF camera poses and rendered videos, into a shared feature representation. This module is able to extract shared camera motion cues, enabling precise pose control while effectively preserving fine visual details from the source video, thereby ensuring high-fidelity generation. Furthermore, we observed that fusing the two control modalities simultaneously can hinder the convergence of the training. To address this, we adopt a two-stage training strategy: first learning basic camera motion solely from poses, and then incorporating rendered videos to achieve finer motion control and enhanced visual fidelity. As shown in Fig. 2, thanks to our innovative approach, we are able to maintain precise motion control while faithfully following the content of the source video, and demonstrate enhanced robustness. Extensive experiments show that PostCam outperforms state-ofthe-art methods by over 20% in camera-control precision and view consistency, achieving the highest VBench composite scores on both real and synthetic datasets. Our contributions are summarized as follows:

- We propose PostCam, a novel-view video generation framework that enables precise post-capture camera control while maintaining high-fidelity synthesis of dynamic scenes. We will release the code and test datasets to support future research.
- We propose a query-shared cross-attention module

that effectively fuses 6-DoF camera poses with rendered videos into a shared feature space, enabling robust motion conditioning and improving spatiotemporal coherence.

- We propose a two-stage training strategy that decouples motion learning from appearance refinement, thus facilitating better network convergence.
- Extensive experiments demonstrate that PostCam outperforms state-of-the-art methods by over 20% in cameracontrol accuracy and view consistency, achieving superior perceptual quality on both real and synthetic datasets.

2. Related Work

2.1. Video Generation.

Our method is built upon the video diffusion model which has emerged as the prevailing paradigm for video generation. VDM [14] pioneered the exploration of diffusion models for high-resolution video generation. In recent years, video diffusion architectures have transitioned from U-Nets [5, 11, 30] to transformer-based designs [6, 18, 32, 38, 44], unlocking better realism and dynamic fidelity. Among them, Wan2.1 [32] demonstrates superior generation capability as an open-source model and is therefore selected as our backbone.

2.2. Camera Controllable Video Generation.

Camera-controllable video generation was initially advanced under the frameworks of text-to-video and imageto-video synthesis. As a pioneering work, MotionCtrl [34] encodes 6DoF camera poses and injects them into the diffusion model, fine-tuning on paired video-camera data to achieve video generation with arbitrary trajectory control. Some subsequent works [1, 2, 12, 19, 21, 33, 37, 43] enhance camera accuracy by introducing Plücker embeddings to represent camera configurations. Nevertheless, enabling the model to learn camera-motion control solely from numerical or Plücker representations is challenging, as it demands cross-modal interaction between visual information and numerical signals. Beyond direct camera-poses conditioning, many approaches [9, 10, 20, 25, 28, 29, 40, 41] instead leverage point-cloud-rendered videos for cameramotion control: monocular depth is first lifted to a 3-D point cloud, after which a proxy video is rendered from the target camera pose and injected into the network as a strong visual constraint. DaS [10] takes this one step further by replacing the RGB render with a 3-D point-trajectory video, endowing the diffusion model with intrinsic 3-D awareness. Some image-to-video works, such as MVGenMaster [7] and Uni3C [8], attempt simple modal fusion. They conventionally inject and combine Plücker coordinates (from camera poses) and rendered video into the latent space using addition and channel-concatenation. Furthermore, several training-free methods have been proposed [15, 16, 22, 36].

Overall, these methods achieve a degree of camera control, yet they remain restricted to reference-image or prompt-based generation and cannot synthesize results conditioned on a given source video.

2.3. Novel-View Video Generation.

Novel-view video generation with camera control has been pursued along two main avenues. Pose-based methods condition a diffusion model on extrinsic camera parameters. GCD [31] pioneers camera-controllable video-tovideo generation by training on synthetically paired data from the Kubric simulator; its performance, however, degrades under the large domain gap between synthetic and real videos. ReCamMaster [3] augments the noised latent with encoded pose vectors, yet the implicit injection inevitably perturbs visual quality. A common limitation of these approaches is the weak cross-modal alignment between purely numerical pose signals and rich visual content, resulting in imprecise trajectories and limited fidelity. Rendering-based methods [4, 24, 35, 39, 42] circumvent direct parameter injection by constructing an explicit 3-D proxy. TrajectoryCrafter [24] lifts the source video into a point cloud via monocular depth estimation, renders a proxy video from the target camera, and uses this rendered video as a strong visual condition. Although impressive control is achieved when the depth map is accurate, depth errors propagate into texture drift or ghosting artifacts that corrupt the final output. The rendering-based methods [4, 24, 35, 39, 42] share the same fragility: imperfect or incomplete point clouds severely degrade video quality. In contrast to our task (which involves re-generating a video from a new viewpoint based on an input video), CameraCtrl II[13] is dedicated to dynamic scene exploration, which it achieves by iteratively generating the next coherent video clip conditioned on the previous one. In summary, pose-based techniques suffer from weak visual-pose alignment, whereas rendering-based ones are critically sensitive to depth accuracy. Both paradigms currently fail to deliver simultaneously robust pose control and high-fidelity results in real-world scenes.

3. Method

3.1. Preliminary: Base Model.

We adopt Wan2.1 [32] as the backbone, a flow matching [23] framework built upon the prevailing diffusion transformer. It comprises three key components: Wan-VAE, a diffusion transformer, and a text encoder.

Given an input video x_0 , the Wan-VAE compresses it into the latent space z_0 . The model learns the conditional distribution $p(z_0|c_{\rm txt})$, where $c_{\rm txt}$ denotes the text prompt. Wan2.1 employs flow matching to define the forward process with straight paths from the data distribution to the

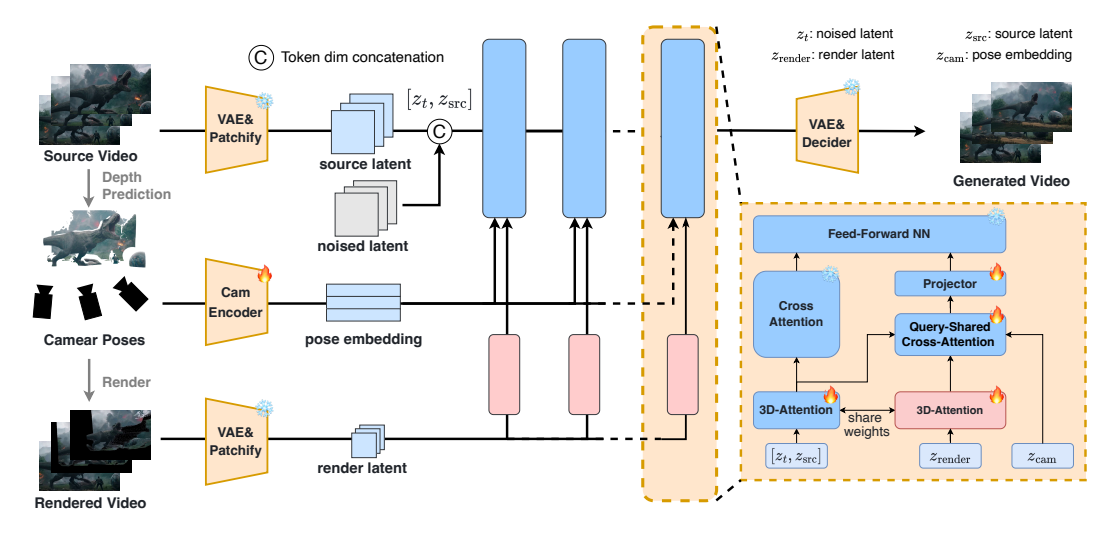


Figure 3. **Framework overview**. The model stacks multiple transformer blocks along three parallel pathways. (a) The source video is first encoded into latent space and then concatenated with noised latents before entering the transformer blocks. (b) the camera parameters are processed by a lightweight encoder and injected into every block via query-shared cross-attention. (c) the rendered video is similarly encoded into latent space; within each block, it undergoes self-attention to extract high-level visual features. An exploded view (bottom right) depicts the internal structure of a transformer block.

standard normal distribution:

$$z_t = (1 - t)z_0 + t\epsilon, \quad \epsilon \sim \mathcal{N}(0, I)$$
 (1)

where t represents the diffusion time step and the noised latent z_t is constructed by randomly adding noise to z_0 . The model predicts the velocity field \mathcal{V}_{θ} through:

$$\min_{\theta} \mathbb{E}_{z_0, t, \epsilon, c_{\text{txt}}} \left[\left\| \mathcal{V}_{\theta}(z_t, t, c_{\text{txt}}) - (\epsilon - z_0) \right\|^2 \right]$$
 (2)

3.2. Overview.

The objective is to learn a model that generates a novel-view target video $x_{\rm tgt}$, conditioned on a source video $x_{\rm src}$ and a target camera trajectory $c_{\rm cam}$. Specifically, we model the conditional distribution $p(z_0 \mid c_{\rm txt}, c_{\rm cam}, z_{\rm src})$, where $z_0 \in \mathbb{R}^{c \times (f \times h \times w)}$ is the latent representation of the target video, $z_{\rm src} \in \mathbb{R}^{c \times (f \times h \times w)}$ is the latent of the source video, $c_{\rm txt}$ denotes the text condition, and $c_{\rm cam}$ represents the camera condition. The symbols c, f, h, and w denote the channel count, temporal frames, spatial height, and width of the latent features after Variational Autoencoder(VAE) encoding and patch tokenization.

As shown in Fig. 3, the text-to-video backbone is extended with three extra inputs: the source video, the camera trajectory, and a rendered video. The source video, serving as a visual reference for both appearance and motion dynamics, is first encoded by a variational autoencoder and to-kenized into patches. The resulting latent representation is concatenated with the noised latent along the token dimension to form $[z_t, z_{\rm src}] \in \mathbb{R}^{c \times (2f \times h \times w)}$, and the concatenated latent is processed by a self-attention mechanism to extract

high-level visual representations. The camera conditions consist of two modalities: the rendering video and the camera trajectory. The proposed query-shared cross-attention injects them jointly into the noisy latent, effectively incorporating camera motion information during denoising.

The training objective is given by:

$$\min_{\theta} \mathbb{E}_{z_0, t, \epsilon, c_{\text{txt}}, c_{\text{cam}}, z_{\text{src}}} \left[\| \mathcal{V}_{\theta}(z_t, t, c_{\text{txt}}, c_{\text{cam}}, z_{\text{src}}) - (\epsilon - z_0) \|^2 \right]$$
(3)

3.3. Camera Condition Preprocessing.

Before injecting the camera conditions into the noised latents, we perform distinct feature-extraction preprocessing for the camera parameters and the rendered video.

For the camera poses, a lightweight camera encoder is trained to map the camera extrinsic matrix \mathbf{c}_{cam} into a pose embedding $\mathbf{z}_{\text{cam}} \in \mathbb{R}^{c \times f}$. To preserve temporal consistency, 1D Rotary Positional Embeddings (RoPE) are applied during the subsequent cross-attention stage.

The rendered video is generated by first lifting the source video into 3D via monocular depth estimation, then reprojecting it along the target camera trajectory. While existing methods rely on full-resolution rendering, we observe that within our query-shared mechanism, the primary role of the rendered video is to refine motion accuracy and enhance visual fidelity, rather than achieving precise pixelwise correspondence. This also explains why the model can still generate correct motion even when inaccurate depth

maps lead to a 'collapsed' (i.e., severely distorted) rendering. Therefore, we downsample the rendered video in the spatial dimensions, reducing computational cost while compromising the quality of the generated output. The downsampled rendered video is encoded together with the source video by the same VAE, after which high-level visual features are extracted through 3D self-attention, resulting in $z_{\text{render}} \in \mathbb{R}^{c \times (f \times \frac{h}{4} \times \frac{w}{4})}$. This self-attention module reuses the weights of the backbone without introducing additional parameters.

3.4. Query-Shared Cross-attention

To suppress extraneous cues from the dual-modality camera condition, we propose a novel query-shared cross-attention module. Within each transformer block, the camera condition is injected into the noised latent via the proposed cross-attention mechanism.

In query-shared cross-attention, the query vector is obtained by applying a linear projection to z_t :

$$Q = \operatorname{Linear}(z_t).$$

Simultaneously, $z_{\rm render}$ and $z_{\rm cam}$ are each linearly projected to generate the corresponding keys ($K_{\rm render}$ and $K_{\rm cam}$) and values ($V_{\rm render}$ and $V_{\rm cam}$).

The keys and values from both conditions are concatenated along the token dimension, and attention is computed as:

$$A = \operatorname{softmax} \left(\frac{Q \left[K_{\text{render}}, K_{\text{cam}} \right]_{\text{token-dim}}^{\top}}{\sqrt{d_q}} \right)$$
 (4)

where d_q is the dimensionality of the query. The module first computes an attention matrix from the query and concat key features. A subsequent softmax operation then generates a weighted distribution, assigning higher importance to features most relevant to the video generation task. These weights govern the selective aggregation of information from the concatenated value features, allowing the module to distill common camera motion cues for both precise pose control and high-fidelity generation. The resulting attention output is projected and added back to the noised latent:

$$z_t = z_t + \text{projector}\left(A\left[V_{\text{render}}, V_{\text{cam}}\right]_{\text{token-dim}}\right)$$
 (5)

3.5. Training Strategy

To preserve the video-generation capability of the base model, almost all of its parameters are frozen. Only the selfattention modules are updated to integrate information from the source latent into the noised latent, ensuring spatiotemporal consistency between them. Additionally, we introduce three trainable modules beyond the base architecture: a camera encoder, a query-shared cross-attention block, and a lightweight projector.

In practice, we adopt a two-stage training strategy that enables the model to better learn low-frequency cameramotion cues while avoiding interference from rendered visual signals during the early training phase: *Stage 1: Pose-Only Conditioning Phase.* In this phase, only the camera extrinsic parameters are used; no rendered video is provided. The camera features are injected as:

$$z_t = z_t + \text{projector}\left(\text{softmax}\left(\frac{QK_{\text{cam}}^T}{\sqrt{d_q}}\right)V_{\text{cam}}\right)$$
 (6)

The projection layer is initialized to zero, effectively suppressing the influence of the camera-control signal during early training. This allows the model to first learn content injection from the source video before acquiring cameramotion control capacity. Without the projector module, the model struggles to converge as it must learn both source injection and camera motion extraction from RT simultaneously. *Stage 2: Joint Conditioning Phase.* In this phase, after the model has acquired coarse camera-control ability, both camera poses and rendered video are provided in training. The model now benefits from the complementary nature of the two conditions, leading to improved control precision and overall generation quality.

4. Experimental Results

4.1. Experimental Setup.

Training Details. For a fair comparison, the model is trained on the same synthetic dataset as RecamMaster [3], using a resolution of 480×832 , 41 frames per video, a learning rate of 1×10^{-5} , and a batch size of 16. The training process consists of two distinct phases. Initially, the model is trained exclusively on camera poses for 7,000 steps, a duration sufficient to achieve initial convergence. Subsequently, the model undergoes a joint training phase for an additional 10,000 steps, utilizing both camera poses and rendered video, until it reaches a final converged state. The additional model parameters introduced are: a linear projector and a cross-attention module within each DiT block, as well as a lightweight camera encoder composed of four linear layers outside the blocks.

Evaluation Dataset. To enable accurate and comprehensive evaluation, we construct real and synthetic test sets. The real-world set includes 100 clips from OpenViD [26], each paired with 10 basic camera trajectories from ReCam-Master, aligning with its testing methods, totaling 1,000 test samples. Since ground-truth videos are unavailable in real-world scenes, we additionally generate a synthetic test set following ReCamMaster's pipeline, enabling a more accurate comparison between the generated and real videos. The synthetic dataset consists of 100 samples from ten dynamic

	Camera Accuracy		Video Quality					View Consistency		
Method	Rot	Trans	Aes.	Img.	Tem.	Motion	Sub.	Bg.	FID↓	FVD↓
	Err↓	Err↓	Qual.↑	Qual.↑	Flick.↑	Smooth.↑	Cons.↑	Cons.↑		
DaS [10]	0.0724	0.4872	52.43	61.69	96.98	98.94	93.39	92.56	101.75	474.29
TrajectoryCrafter [24]	0.0851	0.2154	51.69	59.53	95.31	98.15	90.37	91.28	114.71	478.55
ReCamMaster [3]	0.0649	0.1480	52.23	62.61	96.15	98.89	92.97	91.89	85.68	421.97
PostCam	0.0501	0.1021	53.52	65.71	96.08	99.01	94.03	92.58	67.20	380.96

Table 1. Quantitative comparison with state-of-the-art methods on OpenViD dataset

	Camera Accuracy		Video Quality						View Consistency	
Method	Rot	Trans	Aes.	Img.	Tem.	Motion	Sub.	Bg.	FID↓	FVD↓
	Err↓	Err↓	Qual.↑	Qual.↑	Flick.↑	Smooth.↑	Cons.↑	Cons.↑		
DaS [10]	0.1112	0.9010	49.41	52.62	96.25	98.67	84.55	89.58	363.52	988.56
TrajectoryCrafter [24]	0.0924	0.2653	51.64	50.77	94.11	97.62	83.54	89.50	250.91	799.15
ReCamMaster [3]	0.0638	0.1437	58.50	63.31	95.98	99.08	91.13	91.65	103.74	434.34
PostCam	0.0495	0.0791	59.80	64.64	96.17	99.13	92.48	93.15	80.29	313.02

Table 2. Quantitative comparison with state-of-the-art methods on synthetic datasets

scenes, each rendered along ten random trajectories. Examples of the synthetic test set and more details can be found in the supplementary material.

Evaluation Metrics. (1) Camera Accuracy: To evaluate the camera motion control accuracy of different models, we estimate the camera trajectory of the generated video and compare it with the ground-truth trajectory, computing the rotation error (RotErr) and translation error (TransErr). Since conventional pose estimation methods (e.g., COLMAP and GLOMAP) often fail in dynamic scenes, we evaluated several alternative approaches and ultimately adopted VGGT, a feed-forward reconstruction method that demonstrated more suitable for our experiments. Detailed comparative results of different trajectory estimation methods are provided in the supplementary material. (2) Video Quality: We evaluate the video quality with the widely-used VBench [17] metrics, and report the dimensions of Aesthetic Quality (Aes. Qual.), Imaging Quality (Img. Qual.), Temporal Flickering (Tem. Flick.), Motion Smoothness (Motion Smooth.), Subject Consistency (Sub. Cons.), and Background Consistency (Bg. Cons.). (3) View Consistency: We assess the view consistency between generated and real videos in the feature space using Fréchet Image Distance (FID) and Fréchet Video Distance (FVD). For real-world datasets, we measure the similarity between the generated videos and their corresponding source videos. For synthetic datasets, we compare directly against groundtruth target videos.

4.2. Comparison with State-of-the-Art Methods

We compare with state-of-the-art camera-conditioned video-generation methods: DaS [10], Trajecto-ryCrafter [24], and ReCamMaster [3]; To ensure a

fair evaluation, a unified preprocessing pipeline was applied to all generated videos to standardize spatial resolution and temporal length. Initially, each method generated videos at its officially recommended length, which were subsequently normalized to a uniform duration through frame sampling or truncation. A similar principle was applied for spatial resolution: we ensured that the initial frame for every method contained identical information to prevent extraneous content from causing an unfair comparison.

As demonstrated in Table 1 and Table 2, PostCam substantially outperforms the baseline methods in camera-control accuracy. Simultaneously, it achieves state-of-the-art performance on most video-quality metrics. Qualitative results in Fig. 4 further highlight its advantages. More qualitative comparisons, including examples with OpenVid, synthetic data, and in-the-wild examples, can be found in the supplementary materials Fig. 8, Fig. 7 and supplementary video.

4.3. Ablation Study

4.3.1. Ablation on Conditioning Strategies

To evaluate the impact of different conditioning strategies, we implement the following variants under identical training settings:

- *Pose-only*: Uses only camera parameters as the control signal, injected via cross-attention.
- *Render-only*: Uses only the rendered video, encoded with 3D self-attention and injected via cross-attention.
- Baseline Fusion (RT+Render): Employs both camera parameters and rendered video. Each modality is encoded independently and injected into the network through its own



Figure 4. **Qualitative comparison results.** We compare our method against SOTA (column 3,4,5,6) under specific camera motions (column 2, showing direction and render). Source frames (initial, middle, final) are in column 1. Das, an I2V model, fails to generate coherent results. TrajectoryCrafter, relying on rendering, fails when render data is inaccurate (due to depth errors) or incomplete caused by the source video's own motion (e.g., the missing head in scene 2's final frame). ReCamMaster, though render-agnostic, struggles to achieve both quality and motion precision in difficult scenes. Our method robustly generates high-quality results across all scenes, faithfully aligns with source content and achieves superior pose accuracy.

dedicated cross-attention layer in one stage.

- Baseline Fusion (Plücker+Render): Uses Plücker coordinates and rendered video. Following several image-tovideo (I2V) methods [7, 8] that fuse camera poses and rendered frames, we implement a video-to-video (V2V) version. Specifically, the Plücker information is added to the noised latents and the rendered video is injected through cross-attention in one stage.

Our main model is *PostCam (RT+Render)*. We additionally implement a variant, *PostCam (Plücker+Render)*, which uses Plücker coordinates as input. This variant also adopts the query-shared cross-attention module and the two-stage training strategy.

As shown in Table 3, naively combining the two control signals does not necessarily yield better results. On the contrary, we found that the simple RT+Render strategy struggles to converge and, under the same number of training iterations, results in the worst motion control accuracy. We attribute this to the significant disparity between pose trajectories and rendered video information. Simultaneously injecting these two heterogeneous signals makes the model difficult to optimize. Converting camera poses into Plücker coordinates condition to injection partially alleviates the convergence issue—this also explains why most

Method	Camera	Accuracy	Video Quality		
Wethou	RotErr↓	TransErr↓	Aes. Qual.↑	Img. Qual.↑	
Pose-only	0.0841	0.1545	58.15	63.63	
Render-only	0.0548	0.1786	57.22	62.63	
Baseline Fusion(Plücker+Render)	0.0727	0.2312	58.61	64.95	
Baseline Fusion(RT+Render)	0.1140	0.3718	58.12	62.73	
PostCam(Plücker+Render)	0.0465	0.1259	58.70	64.83	
PostCam(RT+Render)	0.0495	0.0791	59.80	64.64	

Table 3. Ablation study on the synthetic dataset evaluating different camera conditioning methods.

I2V works adopt Plücker coordinates. However, this approach remains a suboptimal injection strategy.

In contrast, our method, utilizing query-shared crossattention, effectively extracts the essential, shared camera motion information from different modalities. This mechanism is agnostic to the pose representation, functioning robustly whether poses are expressed as camera parameters (RT) or Plücker coordinates. As demonstrated in the table, our approach achieves state-of-the-art performance in both camera control accuracy and generation quality.

Specifically, via a single shared query, the model selectively extracts the most beneficial components from both modalities: it first learns fundamental motion patterns solely from camera poses, then incorporates richer visual cues from rendered videos for fine-grained control



Figure 5. Comparisons under different conditions. Our method achieves faithful preservation of fine details and more accurate background generation while ensuring accurate camera motion control. The red boxes highlight that, even when distortions occur in the rendered views, only our results retain fine details, such as the cigarette in the person's hand, while achieving superior pose accuracy.

and quality enhancement. This progressive learning strategy with the shared query mechanism, effectively resolves the aforementioned convergence difficulties and modal conflicts. The qualitative results in Fig. 5 further corroborate our conclusions.

4.3.2. Ablation on query-shared cross-attention

To quantify the contribution of the proposed query-shared cross-attention, we ablate three condition injection strategies while keeping training setting (including two-stage training strategy) and input data identical. w/o queryshared: each transformer block employs two separate crossattention layers, one for camera parameters and another for rendered condition. w/o kv-concatenated: the query matrix is shared, but the keys and values of the two conditions are processed independently and injected into the noise via the same query. ours: the query matrix is shared and the key-value pairs of both conditions are concatenated before attention computation. For a fair comparison, all strategies undergo the same two-stage training pipeline. As Table 4 reports, the proposed query-shared cross-attention achieves the highest camera-motion control accuracy. Benefiting from the proposed shared-query design, the module first computes an attention matrix from the query and concat key features. A subsequent softmax operation then generates a weighted distribution, assigning higher importance to features most relevant to the video generation task.

Method	Camera	Accuracy	Video Quality		
Method	RotErr↓	TransErr↓	Aes. Qual.↑	Img. Qual.↑	
w/o query-shared	0.1386	0.1707	59.13	65.94	
w/o kv-concatenated	0.1389	0.1984	59.33	65.90	
Ours	0.0495	0.0791	59.80	64.64	

Table 4. Ablation study on the synthetic dataset evaluating different attention injection mechanism.

Method	Camera	Accuracy	Video Quality		
Witthou	RotErr↓ TransErr↓		Aes. Qual.↑	Img. Qual.↑	
one stage	0.0578	0.1299	58.98	65.05	
two stage, render-first	0.0991	0.1730	56.89	63.08	
two stage, pose-first	0.0495	0.0791	59.80	64.64	

Table 5. Ablation study on the synthetic dataset evaluating different training strategies.

These weights govern the selective aggregation of information from the concatenated value features, allowing the module to distill common camera motion cues for both precise pose control and high-fidelity generation. Qualitative results can be seen in supplementary material Fig. 9.

4.3.3. Ablation on two-stage training.

To validate the efficacy of the proposed two-stage training, we ablate three strategies: (1) "one stage" that directly trains on both camera-control conditions; (2) "two stage, render-first" that employs only the rendered condition in the first stage and both conditions in the second; and (3) "two stage, pose-first" (i.e., ours) that employs only the pose condition in the first stage and both conditions in the second. As shown in Table 5, our two-stage training achieves the best camera control among the three. In the one-stage case, the model must simultaneously learn multiple control conditions, leading to suboptimal camera-control accuracy. In the render-first two-stage case, the model favors enforcing pixel-level alignment between the rendered frames and the synthesized output, rather than learning the underlying camera motion, resulting in degraded pose controllability. By contrast, our approach enables the model to first learning underlying camera motion from poses alone, and subsequently incorporating rendered videos for finer motion control and enhanced visual fidelity.

5. Conclusion

We propose PostCam, a novel-view video generation framework for dynamic scenes that enables precise post-capture editing of camera trajectories. To address limitations in existing methods such as low camera control accuracy and inadequate detail preservation, we introduce an innovative query-shared cross-attention module combined with a two-stage training strategy, which significantly enhances the model's understanding and manipulation of camera motion. Experiments on both real-world and synthetic datasets demonstrate that PostCam surpasses current SOTA meth-

ods. Notably, it achieves over 20% significant improvement in camera control precision and view consistency, while also delivering the highest video generation quality.

References

- [1] Sherwin Bahmani, Ivan Skorokhodov, Aliaksandr Siarohin, Willi Menapace, Guocheng Qian, Michael Vasilkovsky, Hsin-Ying Lee, Chaoyang Wang, Jiaxu Zou, Andrea Tagliasacchi, et al. Vd3d: Taming large video diffusion transformers for 3d camera control. arXiv preprint arXiv:2407.12781, 2024. 3
- [2] Sherwin Bahmani, Ivan Skorokhodov, Guocheng Qian, Aliaksandr Siarohin, Willi Menapace, Andrea Tagliasacchi, David B Lindell, and Sergey Tulyakov. Ac3d: Analyzing and improving 3d camera control in video diffusion transformers. In *Proceedings of the Computer Vision and Pattern Recognition Conference*, pages 22875–22889, 2025. 3
- [3] Jianhong Bai, Menghan Xia, Xiao Fu, Xintao Wang, Lianrui Mu, Jinwen Cao, Zuozhu Liu, Haoji Hu, Xiang Bai, Pengfei Wan, et al. Recammaster: Camera-controlled generative rendering from a single video. *arXiv preprint arXiv:2503.11647*, 2025. 3, 5, 6
- [4] Weikang Bian, Zhaoyang Huang, Xiaoyu Shi, Yijin Li, Fu-Yun Wang, and Hongsheng Li. Gs-dit: Advancing video generation with pseudo 4d gaussian fields through efficient dense 3d point tracking. arXiv preprint arXiv:2501.02690, 2025. 3
- [5] Andreas Blattmann, Tim Dockhorn, Sumith Kulal, Daniel Mendelevitch, Maciej Kilian, Dominik Lorenz, Yam Levi, Zion English, Vikram Voleti, Adam Letts, et al. Stable video diffusion: Scaling latent video diffusion models to large datasets. arXiv preprint arXiv:2311.15127, 2023. 3
- [6] Tim Brooks, Bill Peebles, Connor Holmes, Will DePue, Yufei Guo, Li Jing, David Schnurr, Joe Taylor, Troy Luhman, Eric Luhman, et al. Video generation models as world simulators. *OpenAI Blog*, 1:8, 2024. 2, 3
- [7] Chenjie Cao, Chaohui Yu, Shang Liu, Fan Wang, Xiangyang Xue, and Yanwei Fu. Mvgenmaster: Scaling multi-view generation from any image via 3d priors enhanced diffusion model. In *Proceedings of the Computer Vision and Pattern Recognition Conference*, pages 6045–6056, 2025. 2, 3, 7
- [8] Chenjie Cao, Jingkai Zhou, Shikai Li, Jingyun Liang, Chaohui Yu, Fan Wang, Xiangyang Xue, and Yanwei Fu. Uni3c: Unifying precisely 3d-enhanced camera and human motion controls for video generation. arXiv preprint arXiv:2504.14899, 2025. 2, 3, 7
- [9] Wanquan Feng, Jiawei Liu, Pengqi Tu, Tianhao Qi, Mingzhen Sun, Tianxiang Ma, Songtao Zhao, Siyu Zhou, and Qian He. I2vcontrol-camera: Precise video camera control with adjustable motion strength. arXiv preprint arXiv:2411.06525, 2024. 3
- [10] Zekai Gu, Rui Yan, Jiahao Lu, Peng Li, Zhiyang Dou, Chenyang Si, Zhen Dong, Qifeng Liu, Cheng Lin, Ziwei Liu, et al. Diffusion as shader: 3d-aware video diffusion for versatile video generation control. arXiv preprint arXiv:2501.03847, 2025. 3, 6

- [11] Yuwei Guo, Ceyuan Yang, Anyi Rao, Zhengyang Liang, Yaohui Wang, Yu Qiao, Maneesh Agrawala, Dahua Lin, and Bo Dai. Animatediff: Animate your personalized texto-image diffusion models without specific tuning. *arXiv* preprint arXiv:2307.04725, 2023. 3
- [12] Hao He, Yinghao Xu, Yuwei Guo, Gordon Wetzstein, Bo Dai, Hongsheng Li, and Ceyuan Yang. Cameractrl: Enabling camera control for text-to-video generation. arXiv preprint arXiv:2404.02101, 2024. 3
- [13] Hao He, Ceyuan Yang, Shanchuan Lin, Yinghao Xu, Meng Wei, Liangke Gui, Qi Zhao, Gordon Wetzstein, Lu Jiang, and Hongsheng Li. Cameractrl ii: Dynamic scene exploration via camera-controlled video diffusion models. arXiv preprint arXiv:2503.10592, 2025. 3
- [14] Jonathan Ho, Tim Salimans, Alexey Gritsenko, William Chan, Mohammad Norouzi, and David J Fleet. Video diffusion models. Advances in Neural Information Processing Systems, 35:8633–8646, 2022. 3
- [15] Chen Hou, Guoqiang Wei, Yan Zeng, and Zhibo Chen. Training-free camera control for video generation. arXiv preprint arXiv:2406.10126, 2024. 3
- [16] Teng Hu, Jiangning Zhang, Ran Yi, Yating Wang, Hongrui Huang, Jieyu Weng, Yabiao Wang, and Lizhuang Ma. Motionmaster: Training-free camera motion transfer for video generation. arXiv preprint arXiv:2404.15789, 2024. 3
- [17] Ziqi Huang, Yinan He, Jiashuo Yu, Fan Zhang, Chenyang Si, Yuming Jiang, Yuanhan Zhang, Tianxing Wu, Qingyang Jin, Nattapol Chanpaisit, et al. Vbench: Comprehensive benchmark suite for video generative models. In *Proceedings of* the IEEE/CVF Conference on Computer Vision and Pattern Recognition, pages 21807–21818, 2024. 6
- [18] Weijie Kong, Qi Tian, Zijian Zhang, Rox Min, Zuozhuo Dai, Jin Zhou, Jiangfeng Xiong, Xin Li, Bo Wu, Jianwei Zhang, et al. Hunyuanvideo: A systematic framework for large video generative models. arXiv preprint arXiv:2412.03603, 2024.
- [19] Zhengfei Kuang, Shengqu Cai, Hao He, Yinghao Xu, Hong-sheng Li, Leonidas J Guibas, and Gordon Wetzstein. Collaborative video diffusion: Consistent multi-video generation with camera control. Advances in Neural Information Processing Systems, 37:16240–16271, 2024. 3
- [20] Teng Li, Guangcong Zheng, Rui Jiang, Tao Wu, Yehao Lu, Yining Lin, Xi Li, et al. Realcam-i2v: Real-world image-tovideo generation with interactive complex camera control. arXiv preprint arXiv:2502.10059, 2025. 3
- [21] Hanwen Liang, Junli Cao, Vidit Goel, Guocheng Qian, Sergei Korolev, Demetri Terzopoulos, Konstantinos N Plataniotis, Sergey Tulyakov, and Jian Ren. Wonderland: Navigating 3d scenes from a single image. In *Proceedings of the Computer Vision and Pattern Recognition Conference*, pages 798–810, 2025. 3
- [22] Pengyang Ling, Jiazi Bu, Pan Zhang, Xiaoyi Dong, Yuhang Zang, Tong Wu, Huaian Chen, Jiaqi Wang, and Yi Jin. Motionclone: Training-free motion cloning for controllable video generation. arXiv preprint arXiv:2406.05338, 2024. 3
- [23] Yaron Lipman, Ricky TQ Chen, Heli Ben-Hamu, Maximilian Nickel, and Matt Le. Flow matching for generative modeling. arXiv preprint arXiv:2210.02747, 2022. 3

- [24] YU Mark, Wenbo Hu, Jinbo Xing, and Ying Shan. Trajectorycrafter: Redirecting camera trajectory for monocular videos via diffusion models. *arXiv* preprint *arXiv*:2503.05638, 2, 2025. 2, 3, 6
- [25] Norman Müller, Katja Schwarz, Barbara Rössle, Lorenzo Porzi, Samuel Rota Bulò, Matthias Nießner, and Peter Kontschieder. Multidiff: Consistent novel view synthesis from a single image. In Proceedings of the IEEE/CVF Conference on Computer Vision and Pattern Recognition, pages 10258–10268, 2024. 3
- [26] Kepan Nan, Rui Xie, Penghao Zhou, Tiehan Fan, Zhenheng Yang, Zhijie Chen, Xiang Li, Jian Yang, and Ying Tai. Openvid-1m: A large-scale high-quality dataset for text-to-video generation. arXiv preprint arXiv:2407.02371, 2024.
- [27] William Peebles and Saining Xie. Scalable diffusion models with transformers. In *Proceedings of the IEEE/CVF inter*national conference on computer vision, pages 4195–4205, 2023. 2
- [28] Stefan Popov, Amit Raj, Michael Krainin, Yuanzhen Li, William T Freeman, and Michael Rubinstein. Camctrl3d: Single-image scene exploration with precise 3d camera control. arXiv preprint arXiv:2501.06006, 2025. 3
- [29] Xuanchi Ren, Tianchang Shen, Jiahui Huang, Huan Ling, Yifan Lu, Merlin Nimier-David, Thomas Müller, Alexander Keller, Sanja Fidler, and Jun Gao. Gen3c: 3d-informed world-consistent video generation with precise camera control. In *Proceedings of the Computer Vision and Pattern* Recognition Conference, pages 6121–6132, 2025. 3
- [30] Uriel Singer, Adam Polyak, Thomas Hayes, Xi Yin, Jie An, Songyang Zhang, Qiyuan Hu, Harry Yang, Oron Ashual, Oran Gafni, et al. Make-a-video: Text-to-video generation without text-video data. arXiv preprint arXiv:2209.14792, 2022. 3
- [31] Basile Van Hoorick, Rundi Wu, Ege Ozguroglu, Kyle Sargent, Ruoshi Liu, Pavel Tokmakov, Achal Dave, Changxi Zheng, and Carl Vondrick. Generative camera dolly: Extreme monocular dynamic novel view synthesis. In European Conference on Computer Vision, pages 313–331. Springer, 2024. 3
- [32] Team Wan, Ang Wang, Baole Ai, Bin Wen, Chaojie Mao, Chen-Wei Xie, Di Chen, Feiwu Yu, Haiming Zhao, Jianxiao Yang, et al. Wan: Open and advanced large-scale video generative models. *arXiv preprint arXiv:2503.20314*, 2025. 2, 3
- [33] Yuelei Wang, Jian Zhang, Pengtao Jiang, Hao Zhang, Jinwei Chen, and Bo Li. Cpa: Camera-pose-awareness diffusion transformer for video generation. *arXiv preprint* arXiv:2412.01429, 2024. 3
- [34] Zhouxia Wang, Ziyang Yuan, Xintao Wang, Yaowei Li, Tianshui Chen, Menghan Xia, Ping Luo, and Ying Shan. Motionctrl: A unified and flexible motion controller for video generation. In *ACM SIGGRAPH 2024 Conference Papers*, pages 1–11, 2024. 3
- [35] Zeqi Xiao, Wenqi Ouyang, Yifan Zhou, Shuai Yang, Lei Yang, Jianlou Si, and Xingang Pan. Trajectory attention for fine-grained video motion control. *arXiv preprint arXiv:2411.19324*, 2024. 3

- [36] Zeqi Xiao, Yifan Zhou, Shuai Yang, and Xingang Pan. Video diffusion models are training-free motion interpreter and controller. arXiv preprint arXiv:2405.14864, 2024. 3
- [37] Dejia Xu, Weili Nie, Chao Liu, Sifei Liu, Jan Kautz, Zhangyang Wang, and Arash Vahdat. Camco: Camera-controllable 3d-consistent image-to-video generation. *arXiv* preprint arXiv:2406.02509, 2024. 3
- [38] Zhuoyi Yang, Jiayan Teng, Wendi Zheng, Ming Ding, Shiyu Huang, Jiazheng Xu, Yuanming Yang, Wenyi Hong, Xiaohan Zhang, Guanyu Feng, et al. Cogvideox: Text-to-video diffusion models with an expert transformer. *arXiv preprint arXiv:2408.06072*, 2024. 2, 3
- [39] Hidir Yesiltepe and Pinar Yanardag. Dynamic view synthesis as an inverse problem. arXiv preprint arXiv:2506.08004, 2025. 3
- [40] Wangbo Yu, Jinbo Xing, Li Yuan, Wenbo Hu, Xiaoyu Li, Zhipeng Huang, Xiangjun Gao, Tien-Tsin Wong, Ying Shan, and Yonghong Tian. Viewcrafter: Taming video diffusion models for high-fidelity novel view synthesis. arXiv preprint arXiv:2409.02048, 2024. 3
- [41] Shangjin Zhai, Zhichao Ye, Jialin Liu, Weijian Xie, Jiaqi Hu, Zhen Peng, Hua Xue, Danpeng Chen, Xiaomeng Wang, Lei Yang, et al. Stargen: A spatiotemporal autoregression framework with video diffusion model for scalable and controllable scene generation. arXiv preprint arXiv:2501.05763, 2025. 3
- [42] David Junhao Zhang, Roni Paiss, Shiran Zada, Nikhil Karnad, David E Jacobs, Yael Pritch, Inbar Mosseri, Mike Zheng Shou, Neal Wadhwa, and Nataniel Ruiz. Recapture: Generative video camera controls for user-provided videos using masked video fine-tuning. In *Proceedings of the Computer Vision and Pattern Recognition Conference*, pages 2050–2062, 2025. 3
- [43] Guangcong Zheng, Teng Li, Rui Jiang, Yehao Lu, Tao Wu, and Xi Li. Cami2v: Camera-controlled image-to-video diffusion model. arXiv preprint arXiv:2410.15957, 2024. 3
- [44] Zangwei Zheng, Xiangyu Peng, Tianji Yang, Chenhui Shen, Shenggui Li, Hongxin Liu, Yukun Zhou, Tianyi Li, and Yang You. Open-sora: Democratizing efficient video production for all. *arXiv preprint arXiv:2412.20404*, 2024. 2, 3